

# Artificial Intelligence Approach to Real-Time Selective Harmonic Elimination in Voltage Source Multilevel Inverter

Adeyemo, I. A., Ojo, J. A., Babajide, D. O.

**Abstract:** Real-time application of Selective Harmonic Elimination-Pulse Width Modulation (SHE-PWM) technique is limited due to the heavy computational cost involved in solving a specified number of transcendental nonlinear equations known as Selective Harmonic Elimination (SHE) equations that contain trigonometric functions. Traditional methods of solving SHE equations include numerical techniques, and derivative free evolutionary algorithms. However, none of these methods can compute the switching angles in real time. In this paper, a two-phase adaptive algorithm is proposed for real-time generation of optimal switching angles in multilevel inverters. In the first phase, optimal switching angles are calculated offline using real coded genetic algorithm (RCGA). In the second phase, results of RCGA are used to train an ANFIS model. Simulation of an 11-level inverter in MATLAB/Simulink reveals that the proposed method is highly efficient for online harmonic reduction in multilevel inverter.

**Keywords:** Multilevel Inverter, Real Coded Genetic Algorithm (RCGA), Adaptive Neuro-Fuzzy Inference System (ANFIS), and harmonics.

## I. INTRODUCTION

With the advent of fast switching semiconductor devices with high power handling capability and the advancement in digital signal processing (DSP), real-time multilevel power conversion has become a rapidly growing area of power electronics with good potential for further development. A multilevel voltage source inverter is a power electronic system that synthesizes a near sinusoidal ac output voltage from different level of dc voltages. The smaller voltage steps yield lower switching losses, improved power quality, lower electro-magnetic interference (EMI), and lower voltage change rate (dv/dt) [1]. The output voltage obtained from a multilevel inverter contains harmonics, which have to be eliminated or minimized for improved performance. To improve converters performance and output power quality, several switching techniques have been proposed for multilevel inverters. These include Sinusoidal Pulse Width Modulation (SPWM), Selective Harmonic Elimination (SHE) method, Space Vector Control (SVC), and Space Vector Pulse Width Modulation (SVPWM) [2], [3].

**Revised Version Manuscript Received on September 29, 2018.**

**Adeyemo, I. A.**, Department of Electronic & Electrical Engineering, Ladoke Akintola University of Technology, PMB 4000, Ogbomoso, Oyo State, Nigeria. E-mail: [iaadeyemo@lautech.edu.ng](mailto:iaadeyemo@lautech.edu.ng)

**Ojo, J. A.**, Department of Electronic & Electrical Engineering, Ladoke Akintola University of Technology, PMB 4000, Ogbomoso, Oyo State, Nigeria. E-mail: [jaajo@lautech.edu.ng](mailto:jaajo@lautech.edu.ng)

**Babajide, D. O.**, Department of Electronic & Electrical Engineering, Ladoke Akintola University of Technology, PMB 4000, Ogbomoso, Oyo State, Nigeria. E-mail: [babajidedemilade@gmail.com](mailto:babajidedemilade@gmail.com)

Selective Harmonics Elimination-Pulse Width Modulation (SHE-PWM) method at fundamental switching frequency however, arguably gives the best result because of its high spectral performance and considerably reduced switching loss. Selective Harmonic Elimination (SHE) or programmed pulse width modulation scheme is a switching technique for inverters that provides direct control over the output waveform harmonics. In this method, the switching angles are chosen (programmed) to eliminate selected harmonics while the fundamental harmonic is satisfied. The implementation of this technique involves solving  $S$  number of transcendental nonlinear equations known as SHE equations that characterize the harmonics in order to eliminate  $(S-1)$  selected low order harmonics. With the increasing number of equations, the inverter voltage waveform approaches a nearly sinusoidal waveform with low harmonic distortion.[2], [3] However, despite its various advantages, the widespread use of SHEPWM is limited due to the heavy computational burden involved in solving SHE equations.

Several methods that have been reported for solving SHE equations can be classified into two groups: The first group is based on deterministic approach using exact algorithms. Newton Raphson iterative method [4] is one of these. The main disadvantage of iterative methods is that they diverge if the arbitrarily chosen initial values are not sufficiently close to the roots. They also risk being trapped at local optima and fail to give all the possible solution sets. Chiassonet *al*[5] proposed a method based on Elimination theory using resultants of polynomials to determine the solutions of the SHE equations. A difficulty with this approach is that as the number of levels increases, the order of the polynomials becomes very high, thereby making the computations of solutions of these polynomial equations very complex. Another approach uses Walsh functions [6], [7], [8] where solving linear equations, instead of non-linear transcendental equations, optimizes the switching angle. The method results in a set of algebraic matrix equations and the calculation of the optimal switching angles is a complex and time-consuming operation.

The second group is based on probabilistic approach using evolutionary algorithms that minimize rather than eliminate the selected harmonics. Evolutionary algorithms such as genetic algorithm [9], particle swarm optimization [10], [11], ant colony system[12], [13], bee algorithm [14] etc are derivative free and are successful in locating the optimal solution,

but they are usually slow in convergence and require much computing time. However, none of either traditional analytical methods or population-based evolutionary algorithms is able to solve SHE equations and generate the required switching angles in real-time. Alternatively, the switching angles are pre-calculated for all the required values of modulation index using either analytical method or evolutionary algorithm, and the obtained results are stored in look-up-tables [15]. This approach called Programmed SHEPWM is very simple but its widespread use is limited due to large amount of memory that is required to store the recalculated switching angles.

In recent years, there is a wide application of artificial intelligence (AI) techniques, such as fuzz logic (FL), artificial neural network (ANN), expert system (ES), and adaptive neuro-fuzzy inference system (ANFIS) in power electronics, motor drives and renewable energy systems due to the flexible nature of the control offered by these techniques. The AI techniques are highly successful in nonlinear systems due to the fact that once properly trained, they can interpolate and extrapolate random data with high accuracy [16].

In this paper, a two-phase optimization algorithm for real-time generation of switching angles in multilevel inverter is presented. The phase-1 uses real coded genetic algorithm (RCGA) for the offline computation of the switching angles in an 11-level inverter at various modulation indices, while phase-2 implements the input-output mapping of modulation index and the desired switching angles using adaptive neuro-fuzzy inference system (ANFIS).

II. MULTILEVEL INVERTER

A. Multilevel Inverter Topologies

The concept of multilevel inverters was developed from the idea of step approximation of sinusoid [17]. Basically, there are three main multilevel topologies. These are Diode-Clamped Multilevel Inverter [18], Capacitor-Clamped Multilevel Inverter [19], and Cascaded H-bridge Multilevel Inverter with separate DC sources [20]. Among the topologies, cascaded H-bridge inverter requires the least number of components, and its modular structure as well as circuit layout flexibility makes it suitable for high voltage and high power applications.

Cascaded H-bridge multilevel inverter is formed by connecting several single-phase H-bridge inverters in series as shown in Figure1 for an 11-level inverter. The number of output voltage levels in a cascaded H-Bridge inverter is given by  $N = 2S + 1$ , where  $S$  is the number of H-bridges per phase connected in cascade. By different combinations of the four switches  $S_1, S_2, S_3,$  and  $S_4$  shown in the Figure1, each H-bridge switch can generate a square wave voltage waveform with different duty cycle on the AC side. To obtain  $+V_{dc}$ , switches  $S_1$  and  $S_4$  are turned on, whereas  $-V_{dc}$  can be obtained by turning on switches  $S_2$  and  $S_3$ . By turning on  $S_1$  and  $S_2$ , or  $S_3$  and  $S_4$ , the output voltage is zero.

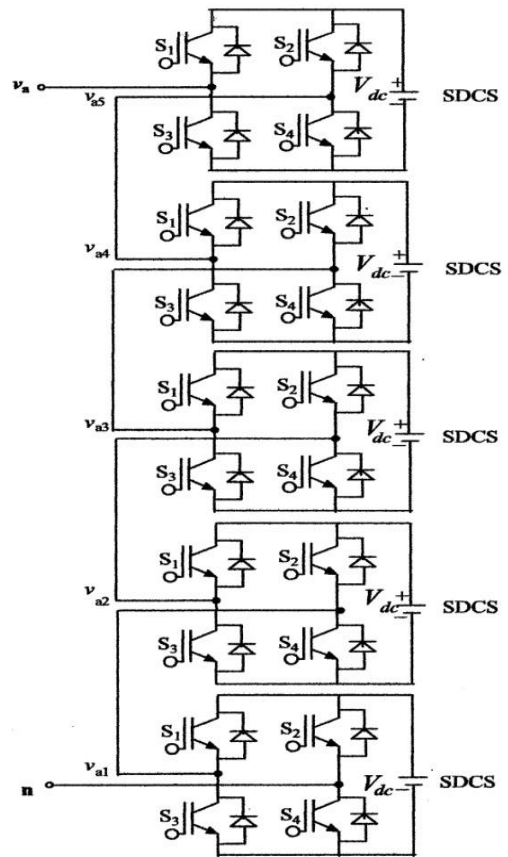


Figure1. Single-Phase Structure of an 11-Levelcascaded H-Bridge Multilevel Converter

The outputs of H-bridge switches are connected in series such that the synthesized AC voltage waveform is the summation of all voltages from the cascaded H-bridge cells [4], [5]. Shown in Figure 2 is the output phase voltage waveform of an 11-level inverter. The magnitude of the ac output phase voltage is given by  $v_{an} = v_{a1} + v_{a2} + v_{a3} + v_{a4} + v_{a5}$  [4]

B. She-Pwmswitching Techniques

Generally, any periodic waveform such as the staircase waveform shown in Figure2 can be shown to be the superposition of a fundamental signal and a set of harmonic components. By applying Fourier transformation, these components can be extracted since the frequency of each harmonic component is an integral multiple of its fundamental [21].

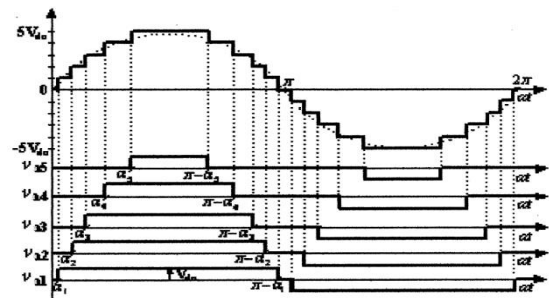


Figure2. Output Voltage Waveform of an 11-Level Inverter.

Assuming quarter-wave symmetry and the equal amplitude of all DC sources, the Fourier series expansion of the staircase output voltage waveform shown in Figure 2 is given by equation (1).

$$V(\omega t) = V_n(\alpha) \sin(n\omega t) \quad (1)$$

Where

$$V_n(\alpha) = \frac{4V_{dc}}{n\pi} \sum_{k=1}^S \cos(n\alpha_k), \text{ for odd } n \quad (2)$$

$$V_n(\alpha) = 0, \text{ for even } n \quad (3)$$

In three-phase power system, the triplen harmonics in each phase need not be cancelled as they automatically cancel in the line-to-line voltages as a result only non-triplen odd harmonics are present in the line-to-line voltages[4]

Combining equations (1), (2) and (3),

$$v(\omega t) = \hat{a}_{n=1,3,5,\dots}^{\neq} \frac{4V_{dc}}{n\pi} (\cos(n\alpha_1) + \cos(n\alpha_2) + \dots + \cos(n\alpha_s)) \sin n\omega t \quad (4)$$

Subject to  $0 < \alpha_1 < \alpha_2 < \dots < \alpha_s \leq \pi/2$

Where,  $S$  is the number of switching angles and  $n$  is the harmonic order. Generally, for  $S$  number of switching angles, one switching angle is used for the desired fundamental output voltage  $V_1$  and the remaining  $(S-1)$  switching angles are used to eliminate certain low order harmonics that dominate the Total Harmonic Distortion (THD) such that equation (4) becomes

$$V(\omega t) = V_1 \sin(\omega t) \quad (5)$$

From equation (4), the expression for the fundamental output voltage  $V_1$  in terms of the switching angles is given by

$$V_1 = \frac{4V_{dc}}{\pi} (\cos(\alpha_1) + \cos(\alpha_2) + \dots + \cos(\alpha_s)) \quad (6)$$

The relation between the fundamental voltage and the maximum obtainable fundamental voltage  $V_{1max}$  is given by modulation index. The modulation index,  $m_i$ , is defined as the ratio of the fundamental output voltage  $V_1$  to the maximum obtainable fundamental voltage  $V_{1max}$ . The maximum fundamental voltage is obtained when all the switching angles are zero [4]. From equation (6),

$$V_{1max} = \frac{4SV_{dc}}{\pi} \quad (7)$$

$$\therefore m_i = \frac{V_1}{V_{1max}} = \frac{\pi V_1}{4SV_{dc}} \quad \text{Consequently,}$$

$$V_1 = m_i \left( \frac{4SV_{dc}}{\pi} \right) \text{ for } 0 < m_i \leq 1 \quad (8)$$

To develop an 11-level cascaded multilevel inverter, five SDCSs are required. The modulation index and switching

angles that result in the synthesis of AC waveform with the least Total Harmonic Distortion (THD) can be found by solving the following transcendental nonlinear equations known as SHE equations that characterize the selected harmonics:

$$\frac{4V_{dc}}{\pi} (\cos(\alpha_1) + \cos(\alpha_2) + \dots + \cos(\alpha_s)) = V_1$$

$$\cos(5\alpha_1) + \cos(5\alpha_2) + \dots + \cos(5\alpha_s) = V_5$$

$$\cos(7\alpha_1) + \cos(7\alpha_2) + \dots + \cos(7\alpha_s) = V_7$$

$$\cos(11\alpha_1) + \cos(11\alpha_2) + \dots + \cos(11\alpha_s) = V_{11}$$

$$\cos(13\alpha_1) + \cos(13\alpha_2) + \dots + \cos(13\alpha_s) = V_{13} \quad (9)$$

In equation (10),  $V_5$ ,  $V_7$ ,  $V_{11}$ , and  $V_{13}$  are set to zero to in order to eliminate 5<sup>th</sup>, 7<sup>th</sup>, 11<sup>th</sup> and 13<sup>th</sup> harmonics respectively. The correct solution must satisfy the condition

$$0 \leq \alpha_1 < \alpha_2 < \dots < \alpha_s \leq \pi/2 \quad (10)$$

Equation (8) in equation (10) yields:

$$\cos(\alpha_1) + \cos(\alpha_2) + \dots + \cos(\alpha_s) = 5m_i$$

$$\cos(5\alpha_1) + \cos(5\alpha_2) + \dots + \cos(5\alpha_s) = 0$$

$$\cos(7\alpha_1) + \cos(7\alpha_2) + \dots + \cos(7\alpha_s) = 0$$

$$\cos(11\alpha_1) + \cos(11\alpha_2) + \dots + \cos(11\alpha_s) = 0$$

$$\cos(13\alpha_1) + \cos(13\alpha_2) + \dots + \cos(13\alpha_s) = 0 \quad (11)$$

Generally equation (12) can be written as

$$F(\alpha) = B(m_i) \quad (12)$$

The Total Harmonic Distortion (THD) is computed as shown in equation (13):

$$THD = \sqrt{\sum_{i=5,7,11,13,\dots}^{49} \left( \frac{V_i}{V_1} \right)^2} \quad (13)$$

### III. REAL CODED GENETIC ALGORITHM

Genetic algorithm (GA) is an evolutionary algorithm that was inspired by the study of genetics and survival of the fittest through the evolution mechanism observed in natural systems and population of living beings. As shown in the flowchart in Figure 3, over successive generations, the parameters of a randomly created initial population of individuals, or potential solutions to the problem called strings or chromosomes are repeatedly modified by GA operators to create new (and hopefully better) population of solutions [22]. Due to the inexact nature of genetic algorithm, its performance depends on the population size as well as the choice and values of the genetic operators used. Population size has to be chosen in such a way that there is balance between the execution time and accuracy, which means that an increase in the accuracy of a solution can only come at the expense of the convergent speed and vice versa.

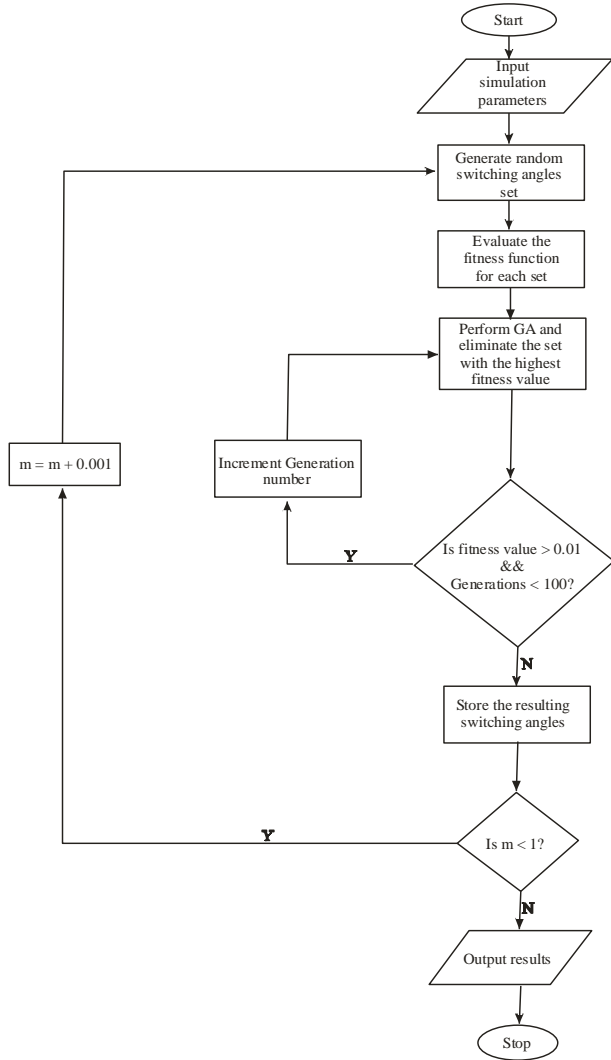


Figure3. Flowchart of Genetic Algorithm

For real valued numerical optimization problems, Real-Coded Genetic Algorithm (RCGA), whose chromosomes comprise real numbers outperforms binary-coded genetic algorithms. The obvious advantages of RCGA include global search capability, enhanced convergent speed resulting from a reduced computational effort (BCGA uses binary code, which needs a lot of time to code and decode the values).

IV. ADAPTIVE NEURO-FUZZY INFERENCE SYSTEM (ANFIS)

Artificial neural network (ANN) and fuzzy logic (FL) are the leading paradigms for modeling nonlinear systems. ANN is an adaptive system that consists of highly connected and parallel nonlinear processing elements that can learn from the knowledge base [23]. It is a powerful technique for mapping input-output nonlinear function; however, it lacks heuristic sense and it works like a black box. On the other hand, FL has the capability of transforming heuristic and linguistic terms into numerical values and vice versa through fuzzy rules and membership function. However, the major drawback of FL is the difficulty involved in finding accurate fuzzy rules and membership functions that are heavily dependent on the prior knowledge of the system [16].

Adaptive neuro-fuzzy inference system (ANFIS) is a hybrid intelligent system that combines the benefits of both artificial neural network (ANN) and fuzzy logic (FL) into a single capsule [24]. ANFIS is simply a soft computing model in which a fuzzy inference system is trained by a neural network learning algorithm. In this way, the low-level learning abilities, connectionist structure and computational power of ANN are brought into fuzzy system while the high-level humanlike IF-THEN thinking and reasoning of fuzzy system are brought into ANN such that IF-THEN rule of FL is used to build a predictive model that maps input to output with high efficiency [25]. Thus, ANFIS can be regarded both as an adaptive fuzzy inference system with capability of learning fuzzy rules from data, and as a connectionist architecture provided with linguistic meaning. ANFIS architecture consists of five layers and its block diagram is shown in Figure 4.



Figure 4. Block diagram of ANFIS structure

A typical ANFIS structure, in which a circle indicates a fixed node while a square indicates an adaptive node, is shown in Figure 5.

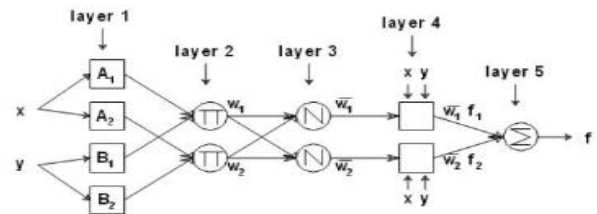


Figure 5. ANFIS Structure for Two Input Variables and Five Layers.

For simplicity, a fuzzy inference system (FIS) with two inputs and one output is considered. For a first-order Sugeno fuzzy model, the rule base contains two fuzzy ‘if-then’ rules that are expressed as follows [25]:

Rule 1: if x is  $A_1$  and y is  $B_1$ , then  $f_1 = p_1 + q_1 + r_1$

Rule 2: if x is  $A_2$  and y is  $B_2$ , then  $f_2 = p_2 + q_2 + r_2$

Where x and y are the crisp inputs, and  $A_i$  and  $B_i$  are the linguistic labels associated with the node function. The output of each node in every layer can be denoted by  $O_i^l$  where  $i$  is the neuron number of the next layer and  $l$  is the prevailing layer number.

The first layer is the fuzzification, which sets and adapts the parameters for the chosen membership functions. Parameters in this layer are called premise parameters. Every node in this layer is an adaptive node and the linguistic labels are  $A_i$  and  $B_i$ . The output of the layer is the membership function of these linguistic labels and is expressed as follows:

For x input to node i,  $O_i^1 = \mu_{A_i}(x)$  For  $i = 1, 2$

For y input to node i,  $O_i^1 = \mu_{B_i}(y)$  For  $i = 1, 2$

Where  $\mu_{A_i}(x)$  and  $\mu_{B_i}(y)$  are membership functions that determine the degree to which the given  $x$  and  $y$  satisfy the quantifiers  $A_i$  and  $B_i$ .

In the second layer, called antecedent rule layer, the firing strength for each rule quantifying the extent to which any input data belong to that rule is calculated. Every node in this layer is a fixed node, whose output represents the firing strength of a rule, and the firing strength represents the IF conditions to set the rules. The output of this layer is the algebraic product of the input signals given as:

$$w_i = \mu_{A_i}(x) \cap \mu_{B_i}(y) \quad \text{For } i=1, 2 \quad (14)$$

In the third layer, called the normalization layer, every node is a fixed node that calculates the ratio of the  $i^{\text{th}}$  rule's firing strength to the sum of all rules' firing strength.

$$\bar{w} = \frac{w_i}{w_1 + w_2}, \quad i=1, 2 \quad (15)$$

The fourth layer called the consequent layer is the adaptation layer of the rules, where the model parameters are tuned to derive the best matching between input and output. Every node  $i$  in this layer is an adaptive node with a node function:

$$O_i^4 = \bar{w}_i f_i = \bar{w}_i (p_i x + q_i y + r_i) \quad (16)$$

Where  $\bar{w}$  is the output of the third layer and  $\{p_i, q_i, r_i\}$  is the parameter set of node  $i$ . These parameters are referred to as consequent parameters. The last layer is the summation layer. It contains a single fixed node labeled  $\Sigma$ , which computes the overall output by summing all incoming signals.

$$O_i^5 = \sum_i \bar{w}_i f_i = \frac{\sum_i w_i f_i}{\sum_i w_i} \quad (17)$$

For the ANFIS structure shown in Figure 5, the only user-specified information is the values of the premise parameters and the input-output training data set. Hence, the output can be written as:

$$f = \bar{w}_1 f_1 + \bar{w}_2 f_2 = \frac{w_1}{w_1 + w_2} f_1 + \frac{w_2}{w_1 + w_2} f_2 \quad (18)$$

## V. IMPLEMENTATION

Using MATLAB software, RCGA algorithm was implemented to compute the optimal switching angles that eliminate 5<sup>th</sup>, 7<sup>th</sup>, 11<sup>th</sup>, and 13<sup>th</sup> harmonics in an 11-level inverter. In this work, the genetic operators adopted are tournament selection, heuristic crossover at the rate of 0.8, and dynamic or non-uniform mutation at the rate of 0.02. The choice of RCGA algorithm's parameters is a tradeoff between accuracy and computational cost. Due to the inexact nature of RCGA algorithm, its parameters were chosen on trial and error basis. Based on the performance evaluation after several trials, the population size in this work is 40 and the number of iterations is 100. Sometimes, RCGA converges to a solution before 100 iterations are completed. In order to improve the convergent speed, iterations are stopped if the result remains unchanged for 50

iterations. The solutions were computed by incrementing the modulation index,  $m_i$  in steps of 0.001 from 0 to 1.

The data set used in the ANFIS modeling comprises of the solution sets computed with RCGA. The data set was divided into three subsets for training, testing, and validating. For ANFIS modeling, the RCGA computed data were divided into training (70%), checking (cross-validation) (15%) and testing (validation) (15%) datasets. As reported in Table 1, several ANFIS models of an 11-level inverter were trained, tested, and evaluated using the same number of membership function (NMF) and other parameters but different combination of input membership function (IMF) and output membership function (OMF) to select the best model. The other parameters of the ANFIS models are shown in Table 2.

**Table 1. Performance Evaluation of Different ANFIS Models of an 11-level Inverter**

IMF	OMF	NMF	R <sup>2</sup>	RSME	MAE
Gaussmf	Linear	50	0.8451	6.7712	0.3478
Gaussmf	Constant	50	0.9827	2.6856	0.1244
Gauss2mf	Linear	50	0.9843	2.5694	0.1217
Gauss2mf	Constant	50	0.9837	2.6296	0.1194
<b>Dsigmf</b>	<b>Linear</b>	<b>50</b>	<b>0.9849</b>	<b>2.5274</b>	<b>0.1169</b>
Dsigmf	Constant	50	0.9831	0.1229	2.6824
Gbellmf	Linear	50	0.9845	2.5785	0.1278
Gbellmf	Constant	50	0.9835	2.6107	0.1149

**Table 2. ANFIS Model Parameter Type and their Values**

Number of nodes	204
Number of linear parameters	50
Number of nonlinear parameters	200
Total number of parameters	250
Number of training data pairs	241
Number of checking data pairs	241
Number of fuzzy rules	50
Input membership function	Gaussmf, Gauss2mf, Dsigmf, Gbellmf
Output membership function	Linear, Constant
Optimization method	Hybrid

Based on the performance evaluation of the ANFIS models as reported in Table 1, the input membership function was chosen to be difference between two sigmoid membership functions while the output membership function was set to linear type. The maximum learning epoch of 100 was chosen.

In this work, the learning algorithm adopted for the adaptation of the parameters in the adaptive network of ANFIS is the hybrid learning algorithm. This algorithm is a combination of least square estimation (LSE) and gradient descent. In this learning algorithm, there are two passes;

The forward and backward passes. In the forward pass of the hybrid learning algorithm, functional signals go forward till layer 4 and LSE is used to tune the consequent parameters. In the backward pass, the error rates propagate backward and the premise parameters are updated by the gradient descent. Both RCGA and ANFIS were developed using MATLAB R2018a. A personal computer (1.7 GHz Intel Core i3 dual processor with 4GB Random Access Memory) running MATLAB R2018a on Windows 10Pro was used to carry out the computations.

In order to demonstrate the generalisation capabilities and efficiency of the ANFIS model, an 11-level single-phase Cascaded H-Bridge inverter was modelled in MATLAB-SIMULINK using Sim Power System block set. In each of the five H-Bridges in the 11-level single-phase Cascaded H-Bridge inverter, 12V dc source is the SDCS, and the switching device used is Insulated Gate Bipolar Transistor (IGBT). Fundamental frequency switching scheme was adopted in this work because of its simplicity and low switching losses. Simulations were performed at an arbitrarily chosen modulation index of 0.922 using ANFIS predicted solution sets. Fast Fourier Transform (FFT) analysis of the simulated phase voltage waveforms was performed to show the harmonic spectra of the synthesized waveforms and the corresponding THD value of each solution set was measured using the FFT block.

VI. RESULTS AND DISCUSSION

Shown in Figure 5 is the plot of switching angles that minimize 5<sup>th</sup>, 7<sup>th</sup>, 11<sup>th</sup>, and 13<sup>th</sup> harmonics in an 11-level inverter. It can be seen from Figure 5 that the feasible solutions at various modulation indices can be broadly classified into three regions: 1) No solution region 2) Single solution region 3) Multiple solution region. In the case of multiple solution sets, the set with the least THD is chosen. The plot of ANFIS estimated switching angles is shown in Figure 5 (b). As can be observed from the THD curves of the solution sets plotted in Figure 6, values of the 49<sup>th</sup> order THD are higher at lower modulation indices while they are considerably reduced at the upper end of modulation index. The plot of 13<sup>th</sup> order THD shows how efficiently the selected harmonics are minimized

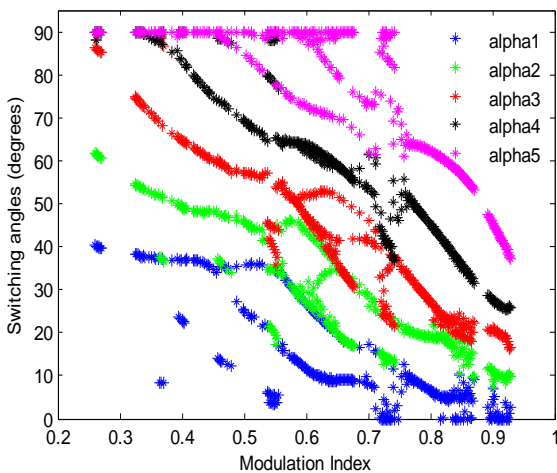


Figure 5 (a). RCGA Computed Switching Angles Versus Modulation Index for an 11-Level Inverter

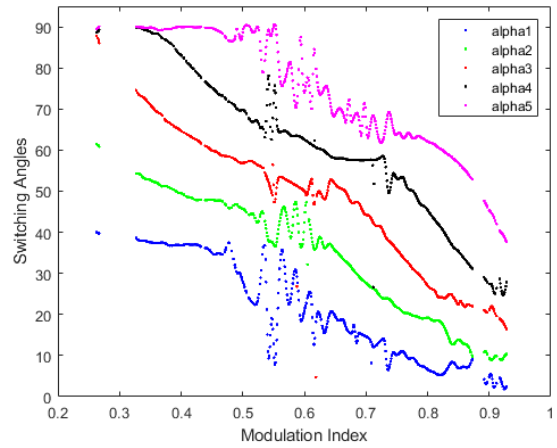


Figure 5(b). ANFIS Estimated Switching Angles Versus Modulation Index for an 11-Level Inverter

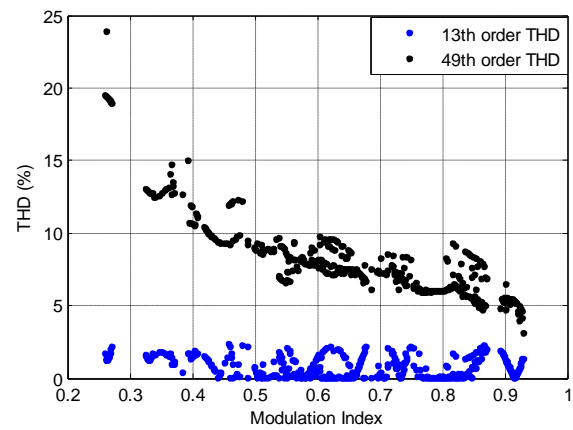


Figure 6. THD Versus Modulation Index for an 11-Level Inverter

At the modulation index of 0.892, ANFIS predicted solution set is [3.4844° 11.3477° 20.8862° 28.6631° 47.6582°], which agrees closely with RCGA computed solution set [4.3417° 10.7361° 20.9512° 28.8261° 47.5657°]. The analytically computed peak value of the fundamental output voltage given by eqn. (8) is

$$V_1 = m_i \left( \frac{4sV_{dc}}{\rho} \right) = 0.892 \left( \frac{4 \times 5 \times 12}{\rho} \right) = 68.18V_{(peak)}$$

This value closely agrees with the simulation value of 68.23V shown in Figure 7. The harmonic spectrum of the synthesized voltage waveform shown in Figure 7 reveals that the selected 5<sup>th</sup>, 7<sup>th</sup>, 11<sup>th</sup> and 13<sup>th</sup> harmonics are well attenuated.

The THD in line-to-line voltage as computed analytically with eqn. (13), and from simulation are 4.75% and 4.26% respectively. It should be noted that the simulation value of THD shown in Figure 7 is 13.09%. This value is for the phase voltage, which includes triplen harmonic components while analytical value is for line voltage which excludes the triplen harmonics.

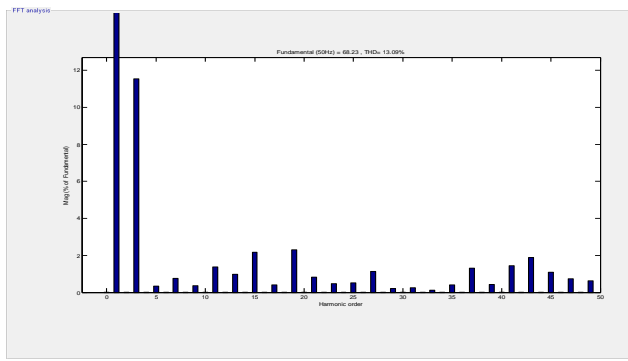


**Figure7. Harmonic spectrum for 11-level inverter at modulation index,  $m_i = 0.892$**

## VII. CONCLUSION

A two-phase algorithm has been successfully implemented for the online generation of switching angles that mitigate lower order harmonics in an 11-level inverter. First, the switching angles are calculated offline, for several depths of modulation, by using real coded genetic algorithm (RCGA) to solve five nonlinear equations simultaneously. Second, these angles are used to train an adaptive neuro-fuzzy inference system (ANFIS) that combines the learning capabilities of artificial neural network and human-like reasoning of fuzzy logic. MATLAB simulations of the trained ANFIS model show that the model works efficiently for online harmonic reduction. The proposed method is adaptive, requires small memory and can be realised with a low-cost microcontrollers for real-time implementation.

## REFERENCES

1. K. A. Corzine, "Multi-Level Converters," The Handbook on Power Electronics, Edited by T.L. Skvarenina, CRC Press, 2002, pp. 6-1 - 6-23
2. J. Rodríguez, J. Lai, F.Peng, "Multilevel inverters: a survey of topologies, controls and applications," IEEE Transactions on Industry Applications, vol. 49, no. 4, Aug. 2002, pp. 724-738.
3. S. Khom foi, L. M Tolbert, Chapter31.Multilevel Power Converters. The University of Tennessee.pp.31-1 to 31-50.
4. J. Kumar, B. Das, and P. Agarwal, "Selective Harmonic Elimination Technique for Multilevel Inverter," 15<sup>th</sup> National Power System Conference (NPSC), IIT Bombay, 2008, pp. 608-613.
5. J. Chiasson, L. M. Tolbert, K. McKenzie, and Z. Du, "Elimination of Harmonics in a Multilevel Converter using the Theory of Symmetric Polynomial and Resultant," Proceedings of the 42<sup>nd</sup> IEEE Conference on Decision and Control, Dec. 2005, pp. 216-223.
6. F. Swift and A. Kamberis, "A New Walsh Domain Technique of Harmonic Elimination and Voltage Control In Pulse-Width Modulated Inverters," IEEE Transactions on Power Electronics, volume 8, no. 2, 1993, pp. 170-185.
7. T. J. Liang and R. G. Hof, "Walsh Function Method of Harmonic Elimination," Proceedings of IEEE Appl. Power Electron.Conference,1993, pp.847-853.
8. T. J. Liang, R. M. O'Connell, R. M. and R. G. Hof, "Inverter Harmonic Reduction Using Walsh Function Harmonic Elimination Method," IEEE Transaction on Power Electron, volume 12, no. 6, 1997, pp. 971-982.
9. B. Ozpineci, L. M. Tolbert, and J. N. Chiasson, "Harmonic Optimization of Multilevel Converters Using Genetic Algorithm," 35 Annual IEEE Power Electronics Specialists Conference, Germany, 2004.
10. N. Vinoth, and H. Umeshprabhu, "Simulation of Particle Swarm Optimization Based Selective Harmonic Elimination," International Journal of Engineering and Innovative Technology (IJEIT) Volume 2, Issue 7, 2013, pp. 215-218.
11. I. A.Adeyemo, O. O. Okediran, and C. A.Oyeleye, "Particle Swarm Optimization Approach to Harmonic Reduction in Voltage Source

12. K. Sundareswaran, K. Jayant, and T. N. Shanavas, "Inverter Harmonic Elimination through a Colony of Continuously Exploring Ants," IEEE Transactions on Industrial Electronics, volume 54, no. 5, 2007, pp. 2558-2565.
13. I. A.Adeyemo, O. A. Fakolujo, and G. A. Adepoju, "Ant Colony Optimisation Approach to THD Analysis in Multilevel Inverter with Different Levels", International Journal of Innovative Research in Science, Engineering and Technology, Volume 4, Issue 9, Sept. 2015, pp. 9071-9082.
14. A. Kavousi, et. al., "Application of the Bee Algorithm for Selective Harmonic Elimination Strategy in Multilevel Inverters," IEEE Transactions on Power Electronics, Vol. 27, No. 4, April 2012, pp.1689-1696.
15. M. Azab, "Harmonic Elimination in Three-Phase Voltage Source Inverters by Particle Swarm Optimization," Journal of Electrical Engineering and Technology, Vol. 6, No. 3, 2011, pp. 334-341.
16. H. Abu-Rub, A. Iqbal, S. M. Ahmed, F. Z. Peng, Y. Li, and G. Baoming, "Quasi-Z Source Inverter-Based Photovoltaic Generation System With Maximum Power Tracking Control Using ANFIS," IEEE Transactions on Sustainable Energy, Vol. 4, No 1, January 2013, pp. 11-20.
17. R. H. Baker and L. H. Bannister, "Electric power converter," U.S. Patent 3867643, Feb. 1975.
18. A. Nabae, I. Takahashi and H. Akagi, "A new neutral-point clamped PWM inverter," IEEE Trans. Ind. Applicant., vol. IA-17, Sept./Oct. 1981, pp. 518-523.
19. T. A. Meynard and H. Foch, "Multi-level conversion: High voltage choppers and voltage- source inverters," in Proc. IEEE-PESC, 1992, pp. 397-403.
20. P. Hammond, "A new approach to enhance power quality for medium voltage ac drives," IEEE Trans. Ind. Applicant., vol. 33, pp. 202-208, Jan./Feb. 1997.
21. S. Sirisukprasert, J. S. Lai, and T. H. Liu, "Optimum Harmonic with a Wide Range of Modulation Indexes for Multilevel Converters," IEEE Transaction on Industrial Electronics, Vol. 49, no; 4, August 2002, pp. 875-881.
22. J. H. Holland, Adaptation in Natural and Artificial Systems (U. Michigan Press, Ann Arbor, Mich., 1975).
23. S. Haykin, Neural Network-A Comprehensive Foundation. 2<sup>nd</sup>ed. New York. Prentice-Hall, 1999.
24. J. S. R. Jang, "ANFIS: Adaptive Network Based Fuzzy Inference System," IEEE Trans. Syst., man., Cybern., Vol. 23, No 3, May/June 1993, pp 665-685.
25. T. R. Sumithira and A. N. Kumar, "Elimination of Harmonics in Multilevel Inverter Connected to Solar Photovoltaic systems Using ANFIS: An Experimental Case Study," Journal of Applied Research and Technology, Vol. 11, No. 1, February 2013, pp. 124-132